JOURNAL OF GEOPHYSICAL RESEARCH, VOL. 115, D06111, doi:10.1029/2009JD012110, 2010

Wetland methane emissions during the Last Glacial Maximum estimated from PMIP2 simulations: Climate, vegetation, and geographic controls

S. L. Weber,[1,2] A. J. Drury,[1] W. H. J. Toonen,[1,2] and M. van Weele[1]

Received 24 March 2009; revised 22 October 2009; accepted 3 November 2009; published 31 March 2010.

[1] It is an open question to what extent wetlands contributed to the interglacial-glacial decrease in atmospheric methane concentration. Here we estimate methane emissions from glacial wetlands, using newly available PMIP2 simulations of the Last Glacial Maximum (LGM) climate from coupled atmosphere-ocean and atmosphere-ocean-vegetation models. These simulations apply improved boundary conditions resulting in better agreement with paleoclimatic data than earlier PMIP1 simulations. Emissions are computed from the dominant controls of water table depth, soil temperature, and plant productivity, and we analyze the relative role of each factor in the glacial decline. It is found that latitudinal changes in soil moisture, in combination with ice sheet expansion, cause boreal wetlands to shift southward in all simulations. This southward migration is instrumental in maintaining the boreal wetland source at a significant level. The mean emission temperature over boreal wetlands drops by only a few degrees, despite the strong overall cooling. The temperature effect on the glacial decline in the methane flux is therefore moderate, while reduced plant productivity contributes equally to the total reduction. Model results indicate a relatively small boreal and large tropical source during the LGM, with wetlands on the exposed continental shelves mainly contributing to the tropical source. This distribution in emissions is consistent with the low interpolar difference in glacial methane concentrations derived from ice core data.

Citation: Weber, S. L., A. J. Drury, W. H. J. Toonen, and M. van Weele (2010), Wetland methane emissions during the Last Glacial Maximum estimated from PMIP2 simulations: Climate, vegetation, and geographic controls, *J. Geophys. Res.*, *115*, D06111, doi:10.1029/2009JD012110.

1. Introduction

[2] Past atmospheric methane (CH_4) concentrations have varied considerably [*Petit et al.*, 1999], showing a decrease by more than 50% from the Pre-Industrial Holocene (PIH; 1850 AD) to the Last Glacial Maximum (LGM; 21,000 years ago). Major reductions in glacial wetland area and associated CH_4 emissions were found in a study based on a vegetation reconstruction for the LGM [*Chappellaz et al.*, 1993]. Other estimates of LGM wetland emissions, based on ice core CH_4 or isotopic composition (top-down modeling), find similar reductions ranging from 40 to 60% [e.g., *Crutzen and Brühl*, 1993; *Martinerie et al.*, 1995]. These studies indicate that the low LGM methane concentration can be explained solely from a decline in the wetland source. A recent top-down study even postulates that the boreal wetland source was completely shut down during the LGM [*Fischer et al.*, 2008]. However, recent bottom-up modeling studies using Earth System Models with atmospheric, vegetation and process-based ecosystem components have found only moderate reductions of 16–29% in LGM wetland emissions [*Kaplan*, 2002; *Valdes et al.*, 2005; *Kaplan et al.*, 2006].

[3] How plausible are these different results? The LGM climate is characterized by a large surface cooling ranging from 2 to 5°C in the tropics [*Farrera et al.*, 1999] to 10–20° C in the Northern Hemisphere (NH) extratropics [*Wu et al.*, 2007], and it is likely that climate is an important driver of wetland emissions. Assuming that the methane flux is reduced by a factor of 2 for each 10°C decrease in temperature [*Cao et al.*, 1996; *Walter et al.*, 2001], temperature effects alone would imply that methane emissions decrease locally by as much as 50–75%. In addition, the area where wetlands can form is reduced during the LGM due to the presence of large continental ice caps.

[4] The present paper addresses the question of whether large changes in climate can be concurrent with moderate changes in total wetland emissions.This is done by analyzing climate model output from eight simulations that have been carried out in the second phase of the Paleoclimate Modelling Intercomparison Project (PMIP2) [*Braconnot et al.*, 2007a]. PMIP2 has used fully coupled atmosphere-

[1]Royal Netherlands Meteorological Institute, De Bilt, Netherlands.
[2]Department of Physical Geography, Faculty of Geosciences, Utrecht University, Utrecht, Netherlands.

0148-0227/10/2009JD012110

Table 1. PIH and LGM Simulations Included in the Analysis, Their Type, Abbreviated Model Names, and Atmospheric Grid Resolution[a]

Model (Country)	Type	Abbreviation	Atmosphere Grid	LGM Mask
HadCM3M2 (UK)	AO	HadCM	3.75 × 2.5	yes
HadCM3M2-TRIFFID (UK)	AOV	HadCM-veg	3.75 × 2.5	yes
CCSM3.0 (USA)	AO	CCSM	2.8 × 2.8	yes
MIROC3.2.2 (Japan)	AO	MIROC	2.8 × 2.8	no
ECHAM-MPIOM127 (Germany)	AO	ECHAM	3.75 × 3.75	no
ECHAM-MPIOM127-LPJ (Germany)	AOV	ECHAM-veg	3.75 × 3.75	yes
IPSL-CM4-V1-MR (France)	AO	IPSL	3.75 × 2.5	yes
CNRM-CM33 (France)	AO	CNRM	2.8 × 2.8	no

[a]Types are atmosphere-ocean (AO) or atmosphere-ocean-vegetation (AOV). Grid resolution is latitude × longitude. LGM Mask indicates whether a specific land-sea mask is used in the LGM simulation.

ocean and atmosphere-ocean-vegetation general circulation models (AO and AOV-GCMs) with a new LGM ice sheet reconstruction (ICE-5G) [*Peltier*, 2004], which resulted in a better match with paleoclimatic data [e.g., *Kageyama et al.*, 2006]. Earlier atmosphere-only PMIP1 simulations, such as used by *Kaplan* [2002] and *Valdes et al.* [2005], have been run with prescribed sea surface temperature reconstructions. Systematic differences with PMIP1 are stronger cooling in the tropics and less continental drying during the LGM in PMIP2 [*Braconnot et al.*, 2007a].

[5] Wetland area and emission strength are estimated in the present study from the simulated LGM and PIH climate, using simple relations derived from the literature. These consist of a wetland location algorithm based on soil moisture and temperature [*Kaplan*, 2002; *Shindell et al.*, 2004] and an expression for the methane flux in terms of the basic climatic controls and substrate availability [*Christensen et al.*, 2003; *Gedney et al.*, 2004]. The latter is taken from those AOV simulations available from the PMIP2 database, which provide LGM and PIH vegetation characteristics on a monthly basis computed from terrestrial ecosystem models. We believe that the present approach is useful as a first-order estimate of the different factors controlling glacial changes in methane production by wetlands. The focus lies on those aspects of climate and vegetation that are most relevant for wetland emissions and we identify signals that are robust among different models.

2. Methods

[6] We selected those AO and AOV-GCMs from the PMIP2 database that have a relatively high spatial resolution, necessary for modeling small-scale features like the occurrence of wetlands (Table 1). Two models were run using both fixed and interactive vegetation (HadCM and ECHAM), whereas the other models used fixed modern vegetation for both time periods. These simulations have been evaluated in various intercomparison studies [e.g., *Kageyama et al.*, 2006; *Braconnot et al.*, 2007a, 2007b; *Weber et al.*, 2007]. All models use identical LGM boundary conditions: the change in solar insolation, reduced greenhouse gas levels and the ICE-5G ice sheet reconstruction. There is some variation between models in the changes in land-sea mask, which are associated with the lowered sea level during the LGM due to the expansion of continental ice sheets. Some of the LGM simulations did not apply a modified land-sea mask (Table 1). For the models where changes are consistent with ICE-5G, there are still small differences in the land-sea mask as model grid resolutions vary. More information on the models and experimental setup can be found on the PMIP2 Web site (http://pmip2.lsce.ipsl.fr/pmip2).

[7] Wetland extent was determined using a wetland location algorithm rather than an inventory based on observations, as there are no inventories available for the LGM. Even for the present day, there is no general agreement on the detailed distribution of wetland area [*Lehner and Döll*, 2004]. Process-based methane emission models [*Cao et al.*, 1996; *Walter et al.*, 2001] have often used the *Matthews and Fung* [1987] inventory, which is based on vegetation type, pond soils and land inundation data. This inventory was found to overestimate boreal wetland area and underestimate tropical wetland area when compared to satellite observations [*Prigent et al.*, 2007]. In addition, the Matthews and Fung estimate probably represents the maximum inundated area, thereby neglecting seasonal dynamics. Wetland location algorithms determine wetlands from climatic (and other) parameters that are known to influence wetland formation. This approach was first applied by *Kaplan* [2002] at 0.5 × 0.5 degree resolution in a global vegetation model forced by meteorological observations. A similar wetland location algorithm was successfully applied by *Shindell et al.* [2004] at 4 × 5 degree resolution in an atmospheric GCM.

[8] Here we will use the same approach, by applying thresholds for soil moisture and temperature on a monthly basis. As wetlands cover only part of a grid cell, it is assumed that slope is not a limiting factor at the grid resolutions of the selected GCMs. Viable wetlands are taken to exist for soil temperature above zero. By trial and error we found threshold values for soil moisture which result in a plausible wetland distribution for all simulations, excluding major deserts and including large parts of the moist tropical region as well as boreal wetlands where snow melt and soil thaw supply sufficient moisture to maintain a positive water balance in summer. Soil moisture was normalized by the global and annual mean value to facilitate comparison between models and the threshold was set at 5–6% (depending on the model). Fractional coverage was taken to increase linearly with soil moisture, ranging between 5.5% of a grid cell and a maximum coverage of 11%. Generally this results in a higher fractional coverage for boreal wetlands than tropical wetlands, which is in agreement with observations [*Matthews and Fung*, 1987; *Prigent et al.*, 2007]. The resulting wetland distributions are evaluated in section 3, taking into account global wetland area, seasonal cycles in different latitude bands and latitudinal distribution.

[9] Methane emissions from natural wetlands basically depend on three factors: soil temperature, water table depth and substrate availability [*Cao et al.*, 1996; *Walter et al.*, 2001; *Kaplan et al.*, 2006]. Here we adopt the simple emission scheme proposed by *Gedney et al.* [2004], which captures these climatic and vegetation controls. The temperature sensitivity is parameterized by a Q_{10} factor. As specific Q_{10} values are only valid for a limited temperature

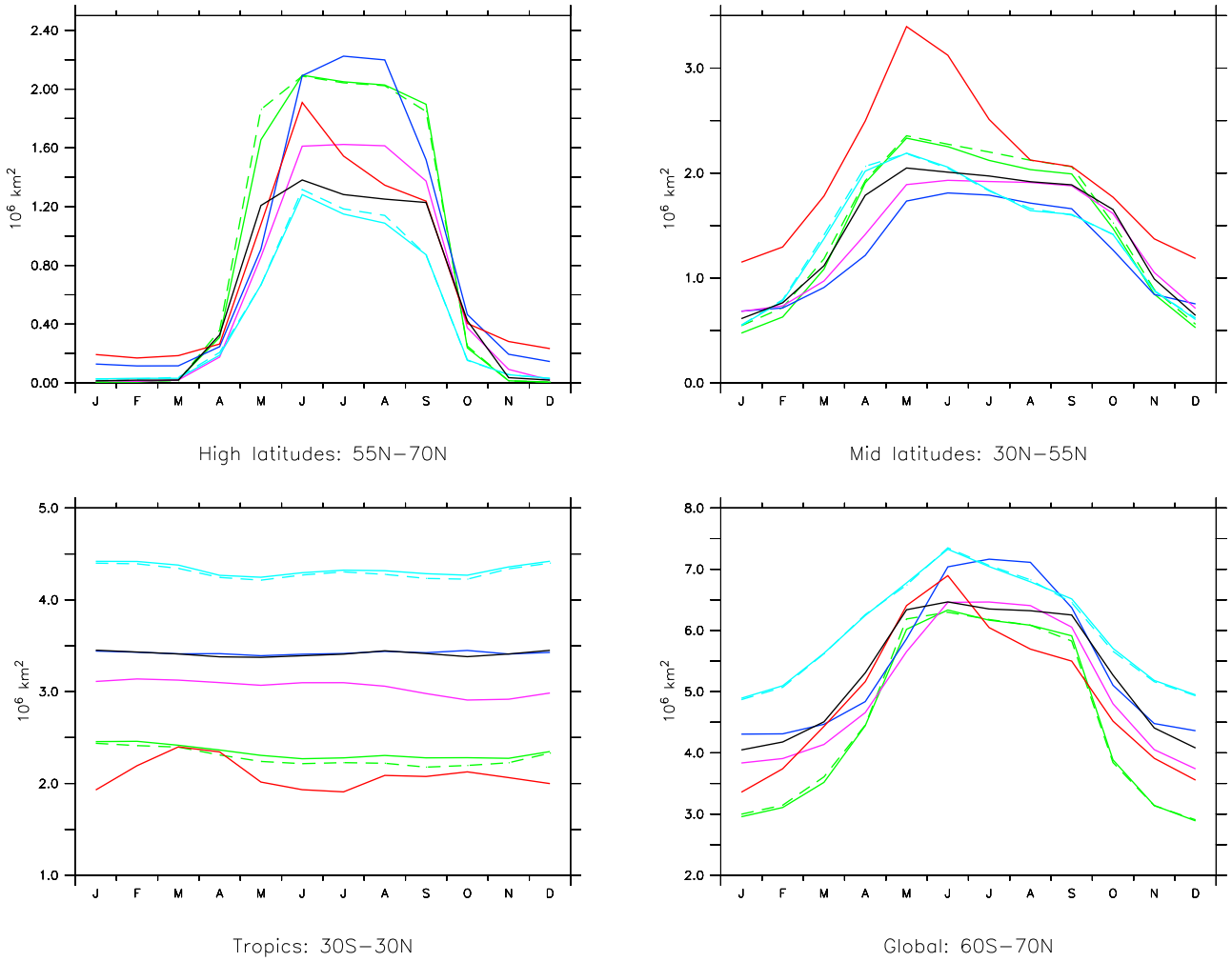

Figure 1. Seasonal variations in PIH wetland area, for different latitude zones and globally, for the eight different PMIP2 simulations: HadCM (green solid line), HadCM-veg (green dashed line), CCSM (pink line), MIROC (dark blue line), ECHAM (light blue solid line), ECHAM-veg (light blue dashed line), IPSL (red line), and CNRM (black line).

range, they take the Q_{10} factor itself to be temperature-dependent in agreement with field data [*Christensen et al.*, 2003]. Application of a similar emission scheme in an inverse atmospheric chemistry transport model resulted in good agreement with satellite observations of atmospheric methane concentrations [*Bergamaschi et al.*, 2007]. Methane is only emitted by that fraction of a grid cell that is effectively wetland, as determined by soil moisture as a proxy for water table depth.

[10] There are two AOV simulations for the LGM and PIH available in the PMIP2 database. These contain ecosystem models (TRIFFID and LPJ; Table 1) which compute spatially explicit and seasonally varying vegetation and their associated carbon and water budgets, forced by climate and atmospheric CO_2 concentration. There is some discussion on which quantity best represents substrate availability for methanogenesis [*Christensen et al.*, 2003]. We choose net primary productivity (NPP) [see *Walter et al.*, 2001; *Kaplan*, 2002; *Valdes et al.*, 2005], rather than carbon content [*Gedney et al.*, 2004], for the pragmatic reason that NPP is available from the PMIP2 database. Simulated changes in NPP are very similar for the two AOV-GCMs. Therefore, the NPP from one model, HadCM-veg, was used in the emission computations for all models.

[11] Combining all components results in the following expression for the emission strength E (in mg/m^2/d):

$$E = k\ C\ NPP\ Q_{10}(T)^{(T-T_0)/10} \quad with \quad Q_{10}(T) = Q_{10}(T_0)^{T_0/T}. \tag{1}$$

Here k is a tunable constant, C is the fractional wetland coverage, T is the soil temperature (in K) and $Q_{10}(T_0)$ is a constant [*Gedney et al.*, 2004]. The reference temperature is defined as T_0 = 273 K. Estimates of the global annual methane flux from wetlands during the PIH vary widely, ranging from 90 Tg [*Cao et al.*, 1996] to 260 Tg [*Walter et al.*, 2001]. We chose a target value of 150 Tg, close to the bottom-up estimate of *Houweling et al.* [2000], and tuned the constant k in (1) to give the required global flux.

[12] The relative distribution of the methane flux over latitude is generally divided into three latitudinal zones; the

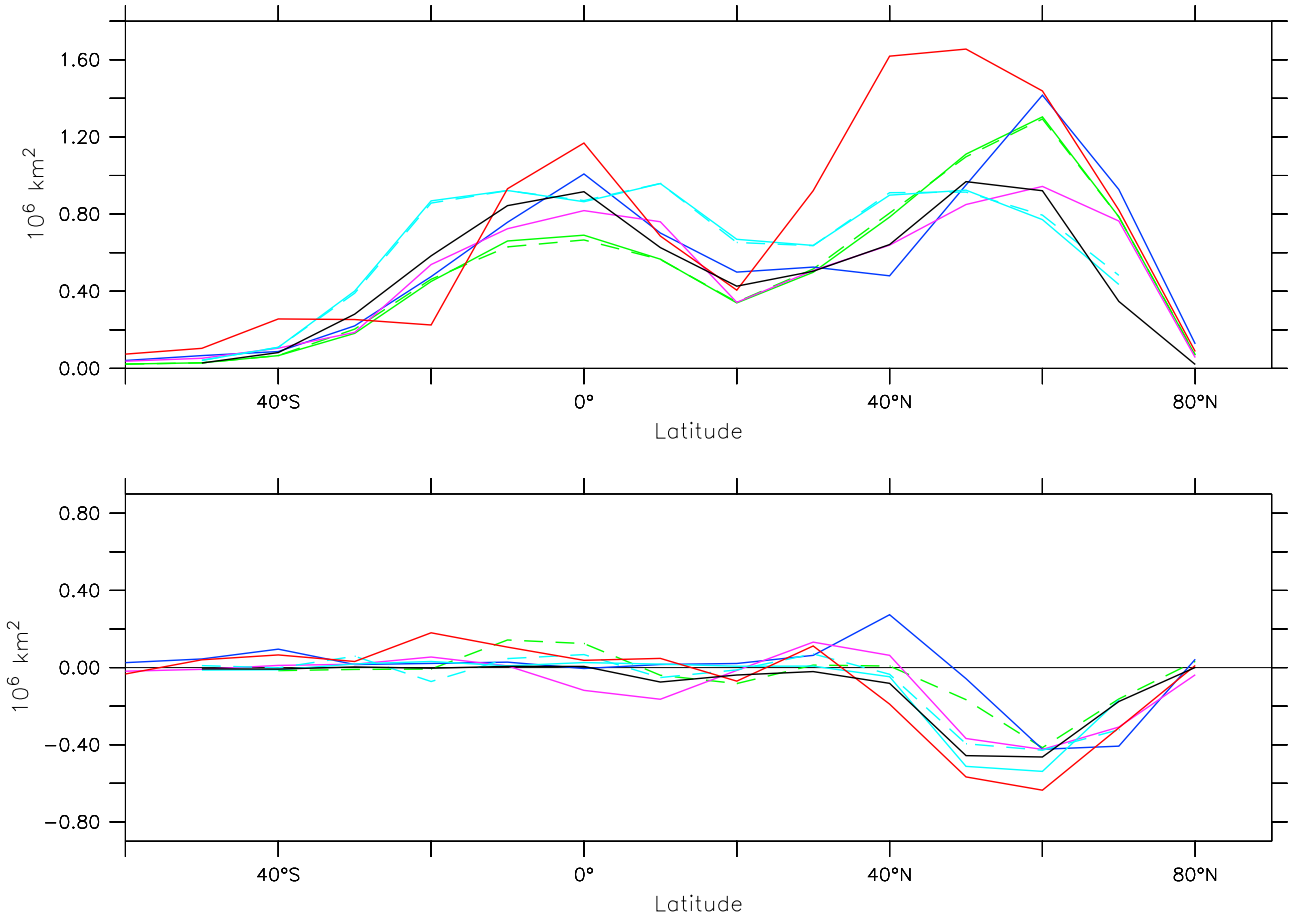

Figure 2. Wetland area for the month of maximum extent, integrated zonally and by 10° latitude belts, for (top) the PH and (bottom) the glacial changes (LGM minus PIH) for the eight PMIP2 simulations. Color code as in Figure 1.

northern extratropics or boreal zone (90°N–30°N), the tropics (30°S–30°N) and the southern extratropics (30°S–90°S). The distribution over these zones is similar for many previous observational and modeling studies, namely 15–37% north, 56–85% tropics and 1–7% south [e.g., *Cao et al.*, 1996; *Walter et al.*, 2001; *Shindell et al.*, 2004; *Valdes et al.*, 2005]. We chose a base $Q_{10}(T_0)$ value so that the latitudinal distribution of simulated emissions agrees with these ranges for all models, given the chosen wetland location algorithm and fractional coverage. This was found to be the case for a $Q_{10}(T_0)$ value of 2.

3. Results

3.1. Wetland Area and Emissions for the PIH and LGM

[13] The simulated global wetland area varies from a minimum of 2.9–4.9 10^6 km^2 to a maximum of 6.5–7.6 10^6 km^2 for the different climate model simulations. This is broadly consistent with estimates based on satellite data of a minimum of 2.1 10^6 km^2 and a maximum of 5.9 10^6 km^2 [*Prigent et al.*, 2007], taking into account that wetland area is assumed to have been ~20% larger during the pre-industrial period than today [*Chappellaz et al.*, 1993]. Seasonal variations are shown globally and by latitude zones in Figure 1. They are very similar to those shown by *Prigent et al.* [2007], with inundated areas going to zero in winter for the high northern latitudes when most surface water is frozen (although peatland complexes themselves do not disappear). Model results do not agree with the data in the tropics where the former show very little seasonality in contrast to the satellite observations. There is, however, pronounced seasonality simulated by all models in smaller regions of the tropics, associated with the occurrence of wet and dry seasons. Due to opposing phases in the northern and southern tropics, this averages out in the simulated total wetland extent over the tropical zone. This inconsistency with modern observations seems partly due to the influence of rice fields, which account for part of the tropical seasonal cycle [*Prigent et al.*, 2007], and these are not considered in the PIH model simulations. Furthermore, differences in spatial distributions of modern and pre-industrial tropical wetlands may play a role.

[14] Viable wetlands exist only during part of the year and this determines the length of the emission season. This varies between 6–12 months in the tropics, where it is determined by the occurrence of wet and dry seasons. It is 3–10 months in the boreal zone, diminishing to 1–2 months at 70°N, reflecting the primary control of temperature on boreal emissions.

Table 2. Annual Methane Emissions From Wetlands During the PIH and the LGM[a]

Model	PIH			LGM		
	Total	90°N–30°N	30°N–30°S	Total	90°N–30°N	30°N–30°S
HadCM	151	41	111	89 (−41%)	17 (−59%)	73 (−34%)
HadCM-veg	145	41	105	85 (−42%)	15 (−63%)	70 (−33%)
CCSM	149	31	119	105 (−29%)	16 (−51%)	90 (−24%)
MIROC	150	37	116	87 (−42%)	15 (−58%)	74 (−36%)
ECHAM	146	21	127	93 (−36%)	8 (−60%)	86 (−32%)
ECHAM-veg	147	21	128	91 (−38%)	10 (−51%)	82 (−35%)
IPSL	150	47	104	97 (−35%)	17 (−64%)	81 (−22%)
CNRM	148	31	119	92 (−38%)	12 (−60%)	81 (−31%)

[a]Shown are global, NH extratropical and tropical values. The numbers in parentheses give the change (LGM minus PIH) as a percentage of the modern value. Emissions are in teragrams.

[15] Generally, simulated wetlands are concentrated in high northern latitudes (40°N–70°N) and a narrow latitudinal belt in the tropics (20°S–20°N) as shown in Figure 2. Insufficient soil moisture obstructs wetland formation in the subtropics. The decrease in wetland extent toward higher latitudes in the southern hemisphere (SH) is due to the decrease in land mass. The exception to this pattern is the IPSL model, which has extensive wetlands in northern midlatitudes and a more narrow tropical zone (Figures 1 and 2). ECHAM results show a relatively large proportion of wetlands (72%) in the tropics, while IPSL and the HadCM runs have the smallest amount of tropical wetlands (45–51%). All other models have two thirds of wetland area in the tropical zone, one third in the boreal zone and less than 1% of total wetland area in the SH extratropics. This distribution is shifted toward the tropics compared to *Matthews and Fung* [1987], consistent with *Lehner and Döll* [2004] and *Prigent et al.* [2007].

[16] Global wetland area during the LGM ranges 2.7–4.8 10^6 km^2 at its minimum to 6.3–7.3 10^6 km^2 at maximum inundation; a decrease by 4–18% compared to the PIH value. Changes in wetland area in the tropics are small and vary among models (Figure 2). Large and consistent changes occur at northern high latitudes, where all models show

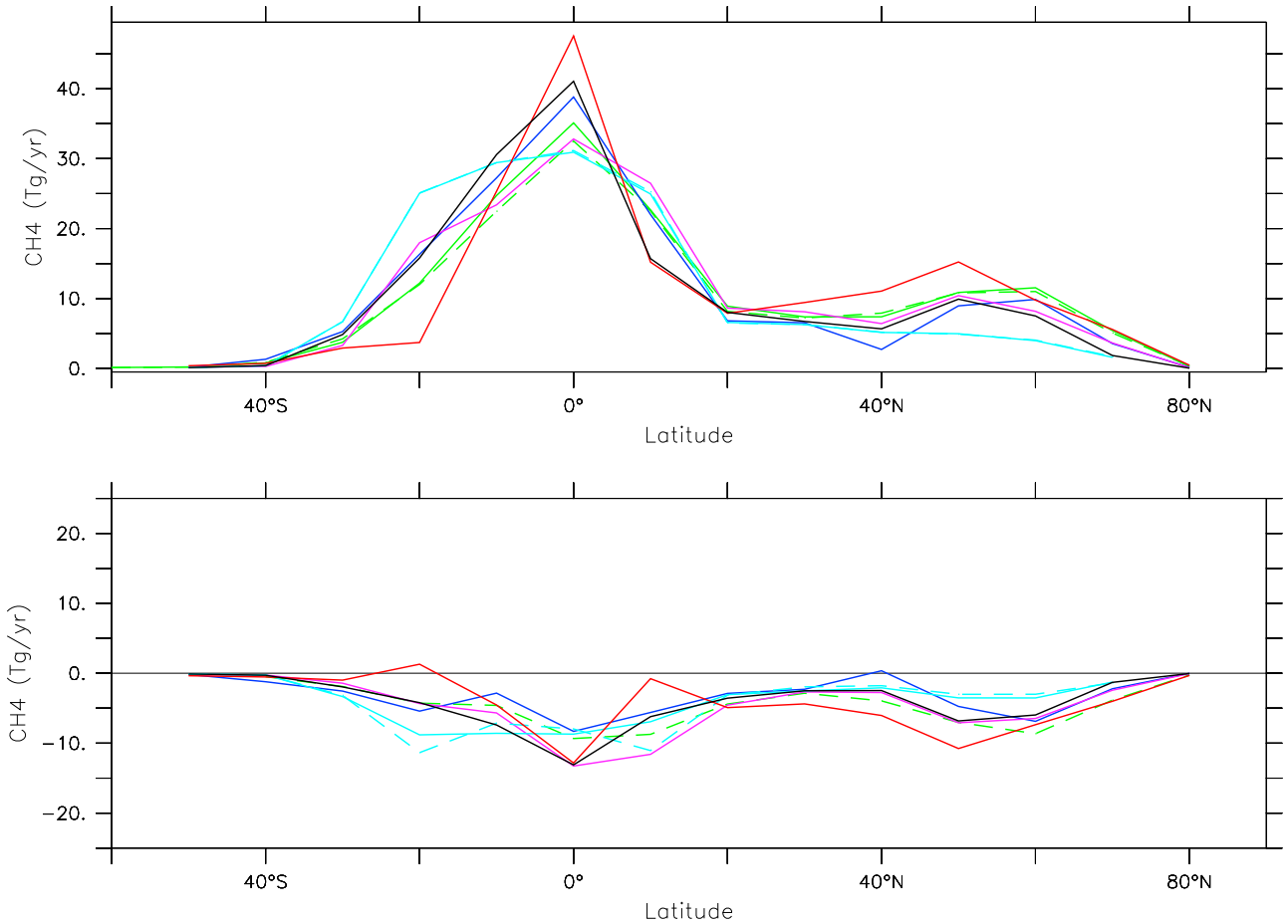

Figure 3. As in Figure 2 but for the annual methane emissions.

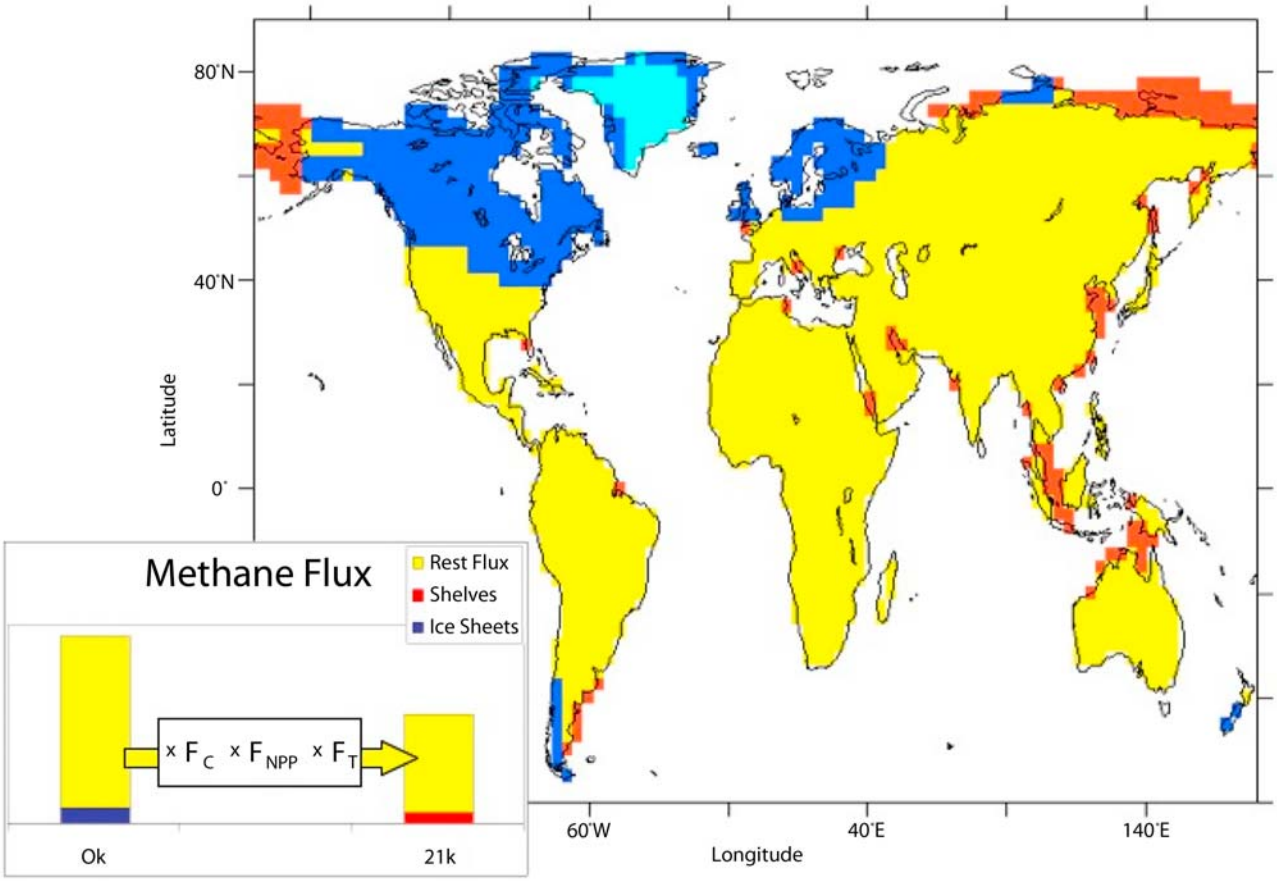

Figure 4. The area where wetlands can potentially form during both the PIH and the LGM is indicated in yellow. Wetlands can only form during the low sea level stand of the LGM in the red area, whereas the dark blue area is covered by ice during the LGM. The light blue area indicates ice during both the PIH and LGM. The factor analysis (section 3.2) examines changes in the methane flux over the yellow area due to wetland coverage, NPP, and temperature, as indicated in the inset.

a major decrease (Figure 2). This is partly due to the expansion of the ice sheets over North America and Europe, resulting in a substantial reduction in potential wetland area. At the same time, wetlands can form during the LGM on newly exposed continental shelves. The effect of these changes in potential wetland area on methane emissions will be discussed further in section 3.2.

[17] The global methane flux was constrained to be ~150 Tg during the PIH (it ranges from 145 to 151 Tg; see Table 2). The latitudinal distribution shows a minor peak between 40°N–60°N and a major peak around the equator (Figure 3). Emissions from latitudes south of 30°S are negligible. The northern and tropical peaks in emissions reflect the corresponding peaks in wetland area, but modified by the different local emission strengths: boreal wetlands are less efficient because of lower temperatures and lower NPP values. Tropical emissions contribute 70–80% to the global methane flux for all models, except for the ECHAM runs. The latter have 87% of their emissions in the tropics, due to the larger tropical wetland area in these simulations.

[18] Compared to the PIH, the LGM methane emissions show an overall decrease by 29–42% (Table 2). The smallest reductions are found in CCSM and IPSL, which both have relatively small reductions in tropical emissions. Disregarding these two outliers, we find that tropical emissions are consistently reduced by about one third (35–46 Tg). Simulated reductions in boreal emissions are larger in a relative sense, ranging 51–65%, but smaller in absolute sense (11–30 Tg).

3.2. Factor Analysis of LGM Methane Emissions

[19] The reduction in methane emissions during the LGM can be due to climatic factors, temperature and soil moisture, changes in vegetation (NPP) and geographic effects such as where continental ice caps cover potential wetland area and new wetlands forming on the exposed continental shelves. The geographic effects are separated from the climatic and vegetation effects by considering only those grid points where wetlands can potentially form during both time periods (Figure 4, yellow), thereby excluding the area covered by ice during the LGM (Figure 4, dark blue) and the land that is below sea level during the PIH (Figure 4, red). Methane emissions from the latter two areas are indicated as E_{ice} and $E_{shelves}$. For the remaining area a total reduction

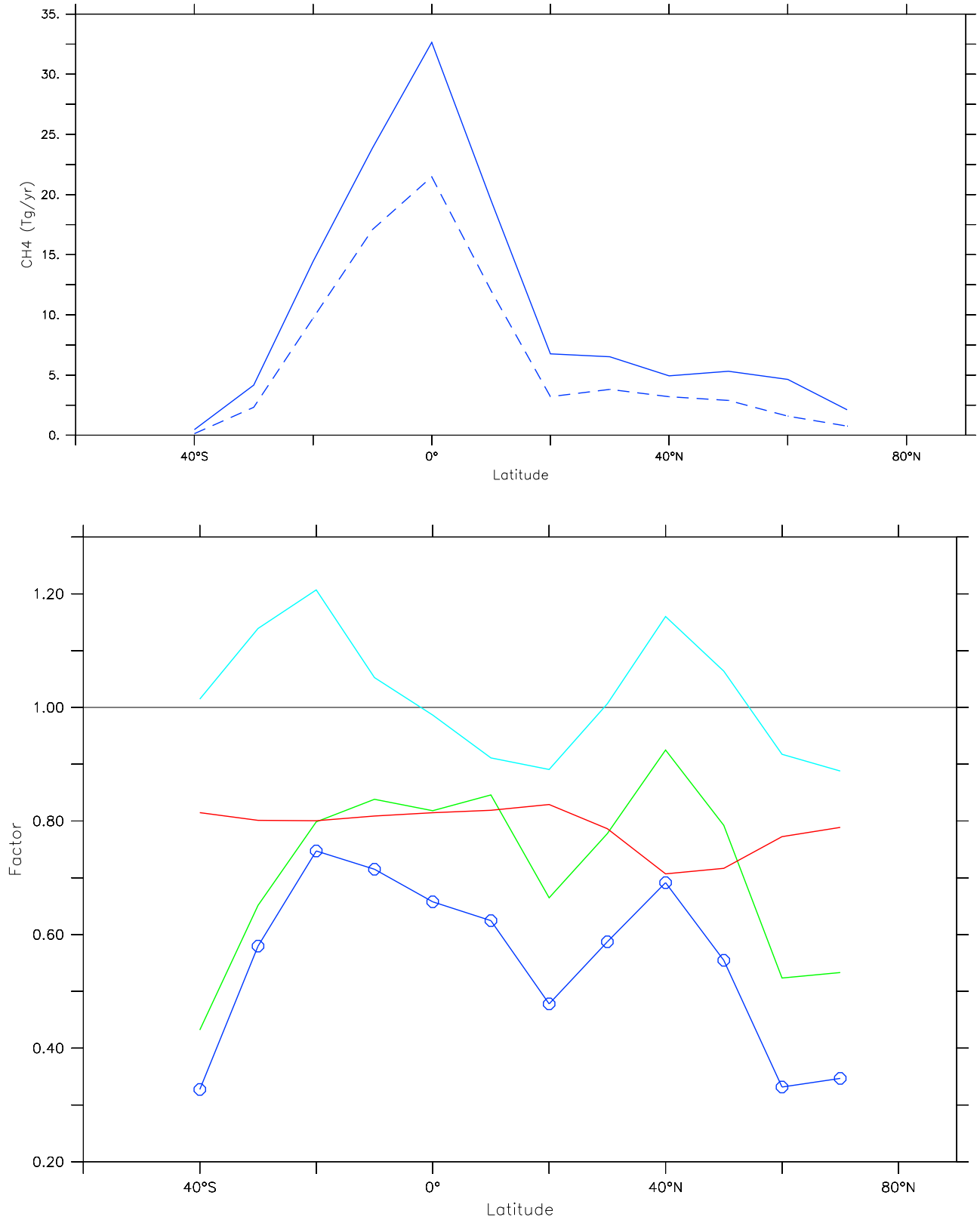

Figure 5. (top) The model-mean annual wetland emissions for the PIH (solid line) and LGM (dashed line) over the "common" area (yellow in Figure 4), integrated zonally and by 10° latitude belts. (bottom) The reduction factors, defined in section 3.2. These are the ratio between LGM and PIH emissions (dark blue, with circles) and the separate factors associated with wetland distribution (light blue line), NPP (green line), and temperature (red line).

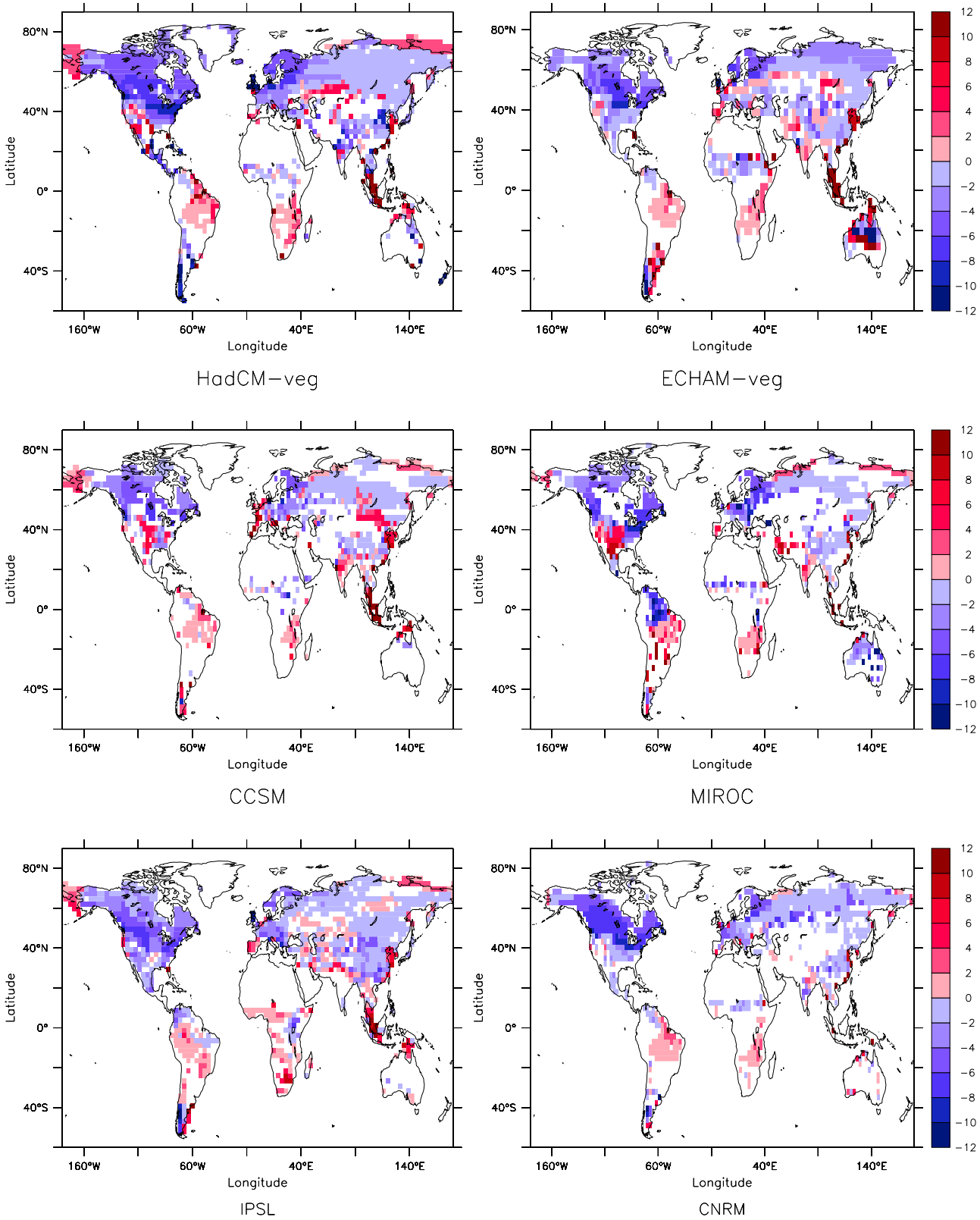

Figure 6. Changes in the length of the emission season (LGM minus PIH, in months) for six PMIP2 simulations. Results for HadCM-veg and ECHAM-veg are very similar to those of the corresponding runs without interactive vegetation.

Table 3. Results of the Factor Analysis[a]

Model	F_{tot}	F_C	F_{NPP}	F_T	Ice	Shelves
HadCM	0.57	0.99	0.77	0.77	−13	10
HadCM-veg	0.57	1.03	0.78	0.73	−13	9
CCSM	0.71	1.00	0.83	0.84	−7	4
MIROC	0.61	0.94	0.79	0.83	−8	0
ECHAM	0.66	1.04	0.81	0.78	−5	0
ECHAM-veg	0.59	0.95	0.82	0.77	−5	8
IPSL	0.62	1.06	0.77	0.78	−16	14
CNRM	0.66	0.98	0.79	0.85	−7	0
Model mean	0.62	1.00	0.80	0.80	−11	9

[a] F_{tot}, F_C, F_{NPP}, and F_T give the multiplicative factors: the ratio F_{tot} between the LGM and PIH wetland source (computed over the yellow "common" area in Figure 4) and the separate reduction factors F_C, F_{NPP}, and F_T associated with wetland distribution, NPP, and temperature. Ice and Shelves give the additive factors: the loss in methane flux due to ice sheets and gain from wetlands on newly exposed shelves, respectively (both in teragrams). Factors are defined in section 3.2.

factor F_{tot} is computed as the ratio of the LGM and PIH methane fluxes,

$$E^{21k} - E^{21k}_{shelves} = F_{tot}\ \left(E^{0k} - E^{0k}_{ice}\right). \quad (2)$$

The total reduction factor F_{tot} can be computed directly from the emission expression (1). Combining (1) and (2) it follows that $F_{tot} = F_C\ F_{NPP}\ F_T$, as indicated in the inset of Figure 4. Here F_C denotes the effect of changes in wetland distribution as determined by soil temperature and moisture changes, F_{NPP} denotes the effect of changes in NPP, and F_T contains the effect of changes in soil temperature through the Q_{10} term. Each separate reduction factor is calculated by dividing the LGM emission by the emission computed with either the wetland coverage (F_C) or NPP (F_{NPP}) or the temperature (F_T) taken at the PIH value rather than the LGM value.

[20] Reduction factors for the zonally integrated annual methane emissions are shown in Figure 5. Results were very consistent between models, therefore we only show the model-mean factors. The wetland coverage factor F_C fluctuates around 1, displaying a southward shift of boreal wetlands as well as of tropical wetlands. The boreal shift in wetland distribution is mainly due to soil moisture effects, with temperature effects causing a small overall decrease in wetland area and thus in emissions. Soil moisture decreases in high northern latitudes and increases at latitudes around 40°N, which is due to a southward displacement of the westerlies by the Laurentide and Fennoscandian ice sheets and a southward extension of snow and soil freeze in winter. This southward shift of wetlands is not as visible in the maximum extent (Figure 2) as it is in the length of the emission season, which becomes shorter at high northern latitudes and longer on the southern margin of the boreal wetland zone (Figure 6). This pattern is clearly visible in all simulations, although spatial details vary considerably among models. Models thus simulate a southward shift in soil moisture and negligible overall drying over the NH extratropics, which is supported by precipitation reconstructions for the LGM which do not significantly differ from the present for Eurasia [*Wu et al.*, 2007] and indicate clearly wetter conditions than today in southwestern North America [*Thompson and Anderson*, 2000]. Lake status data indicate generally wetter conditions than today at 30°N–40°N, in particular in southwestern North America, southern Europe and central Asia [*Kohfeld and Harrison*, 2000].

[21] In the tropical zone F_C also displays a southward shift, related to a southward shift of the ITCZ. This is mirrored in changes in the length of the emission season. The southward shift of the ITCZ, which is found in most PMIP2 simulations of the LGM, is consistent with marine data [*Braconnot et al.*, 2007b]. Continental data indicate both dryer and wetter conditions [*Farrera et al.*, 1999; *Kohfeld and Harrison*, 2000; *Wu et al.*, 2007], depending on site location and altitude. The global mean effect of changes in wetland distribution is a F_C value of 1, varying between 0.94 and 1.06 for the different models (Table 3).

[22] The reduction factor F_{NPP}, related to plant productivity, shows an intricate latitudinal pattern. NPP decreases everywhere, but the reduction is strongest in the NH high latitudes and subtropics and it is smallest around 40°N. There is a similar southward shift in boreal vegetation zones as seen in boreal wetlands. Such a southward displacement of biome types is a well-documented feature of the glacial climate. In the tropics there is a more homogeneous reduction. The global and model-mean reduction is 0.8, varying over a small range (0.77–0.83) for the different simulations (Table 3). The primary cause of lower global mean plant productivity during the LGM seems to be the low atmospheric CO_2 concentration, rather than climatic changes [*Kaplan*, 2002].

[23] Temperature effects reduce methane emissions most around 40°N and are fairly constant everywhere else. The global and model-mean value is 0.8. Model results for F_T are somewhat more variable than for F_{NPP} with a range of 0.73–0.85. The impact of temperature changes is surprisingly small, given the large glacial cooling. It is also surprisingly homogeneous over latitude, considering the pronounced latitudinal gradient in the glacial cooling. Model results for the change in annual temperature between the LGM and PIH are shown in Figure 7. The amplitude of simulated temperature changes is consistent with reconstructions based on proxy data [*Farrera et al.*, 1999; *Wu et al.*, 2007].

[24] However, the annual temperature is not the relevant parameter determining methane emissions. Rather, this is the mean temperature during those months that wetlands exist, as determined by the thresholds for temperature and soil moisture. This mean emission temperature is shown in Figure 7 as well. In the boreal zone the mean emission temperature decreases by only a few degrees. North of 50°N the model-mean cooling is even close to zero, because here the emission season becomes shorter and emissions take place during the warmest months of the year only. Around 40°N the mean emission temperature decreases more, because here the emission season extends into the early and late summer during the LGM as compared to the PIH. Averaged over all boreal wetlands, the mean emission temperature decreases by 0.2–2.7°C in the different simulations. In the tropical zone there is a homogenous decrease in the mean emission temperature that is not much different from the decrease that is seen in the annual temperature

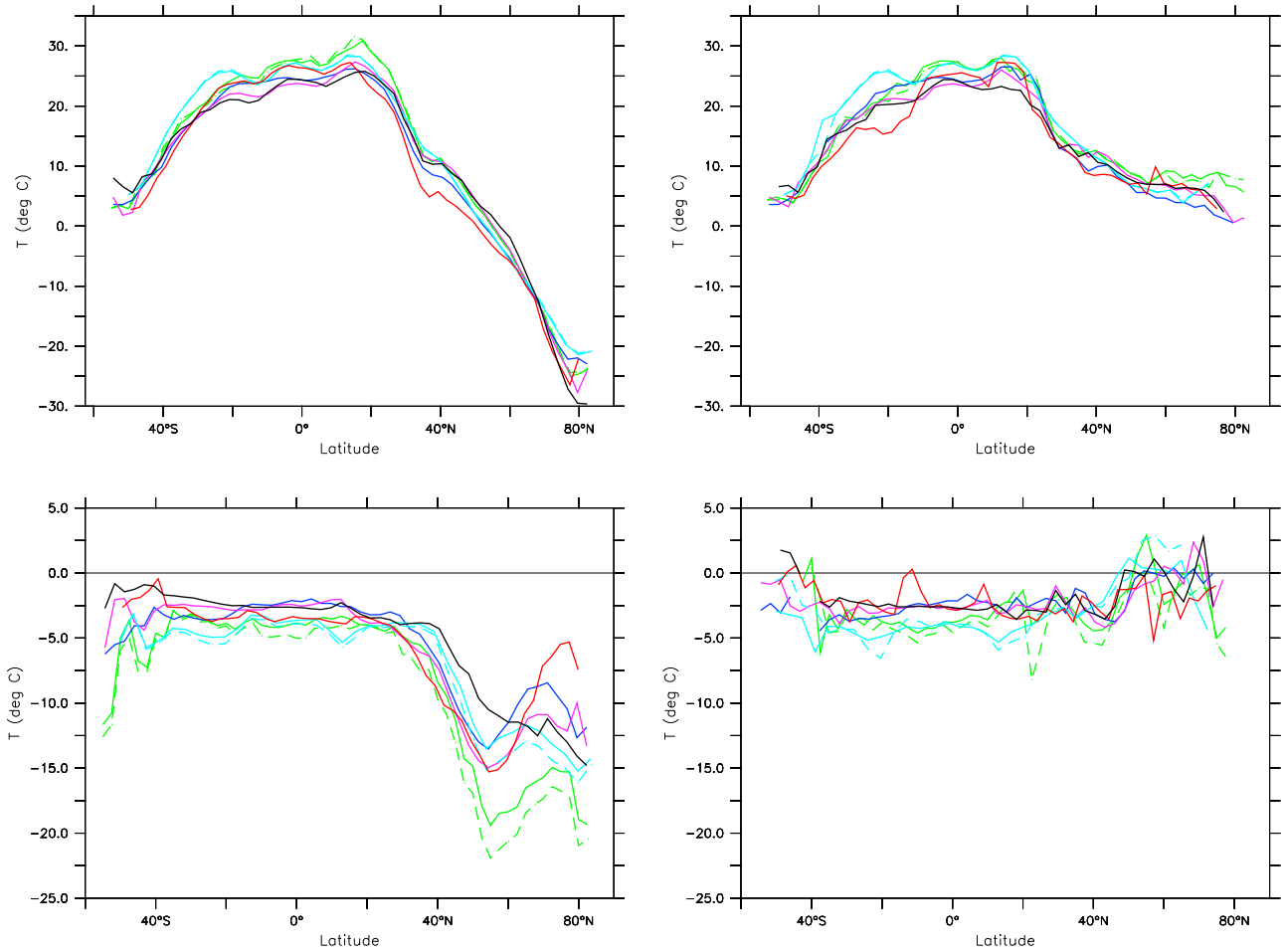

Figure 7. (top left) Annual temperature and (top right) mean emission temperature during the PIH and changes (LGM minus PIH) for the (bottom left) annual temperature and (bottom right) mean emission temperature. Color code as in Figure 1. All values are zonally averaged over land points. The emission temperature is computed as the average during those months of the year that wetlands exist, over land points which are wetland during at least 1 month per year.

(Figure 7). Averaged over the whole tropical zone, the mean emission temperature decreases by 2.6–4.5°C.

[25] Combining all factors, we see a model-mean global reduction in methane emissions by 38% (F_{tot} = 0.62) over the area where wetlands can exist both during the LGM and PIH. Remarkably, temperature effects and vegetation effects contribute equally to this reduction. The globally integrated effect of changes in wetland distribution varies among models but cancels in the model mean, although shifts in wetland coverage can locally result in large changes in emissions. Model results for F_{tot} vary somewhat, with a relatively high value (small reduction) in the CCSM simulation. This is a combination of smaller effects, such as moderate cooling, which causes the simulated relatively small decrease in the global methane flux. The mean emission temperature decreases less in CCSM than in most other models, namely 0.3°C over boreal wetlands and 2.5°C over tropical wetlands.

[26] In addition to the three multiplicative factors, two additive factors play a role in equation (2). These additive components are related to the ice sheets and the exposure of continental shelves during the LGM. The first results in a model-mean reduction in the methane flux by 11 Tg, while the second results in a mean gain by 9 Tg (ignoring simulations that did not modify their land-sea mask for the LGM; Table 3). Values vary substantially among models, with the largest contribution from these geographic factors found in the IPSL model. The reduction due to the presence of the ice sheets is confined to the boreal zone, whereas the "new" wetlands emit methane primarily in the tropics (Figure 8). The combined effect results in a small net loss, but this differs between models with one model (ECHAM-veg) even finding a small net gain. Compared to the temperature and vegetation effects, the net effect of these geographic factors is small. However, the shift in latitudinal distribution of methane emissions from the boreal zone to the tropical zone is largely due to these geographic factors.

4. Discussion and Conclusions

[27] The LGM global methane flux from natural wetlands is consistently reduced by 35–42% in the PMIP2 simulations, with one model finding a somewhat smaller reduction due to moderate cooling. Temperature effects and vegetation

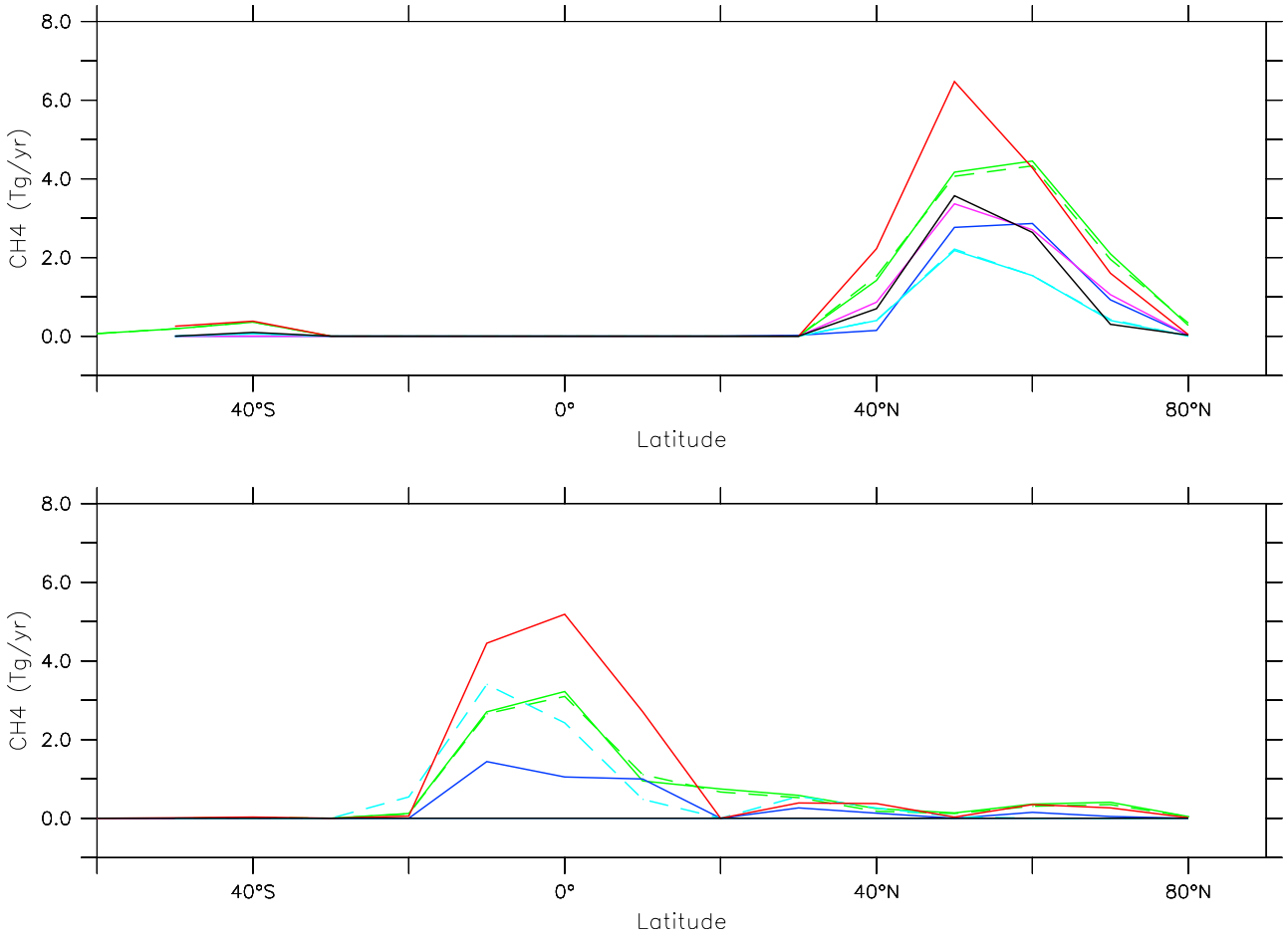

Figure 8. (top) Annual methane emissions from PIH wetlands that were covered by ice during the LGM (dark blue area in Figure 4) and (bottom) from LGM wetlands on continental shelves that are inundated during the PIH (red area in Figure 4). Color code as in Figure 1. Emissions are integrated zonally and by 10° latitude belts.

effects are found to contribute equally to this glacial decline in the wetland source. The pronounced glacial cooling in the NH extratropics is thus seen to be rather ineffective in reducing wetland methane emissions. This lack of effectiveness is due to a southward shift of boreal wetlands and a larger emission season in the southern boreal zone during the LGM compared to the PIH. The mean emission temperature in the boreal zone thus decreases by a few degrees only, comparable in magnitude to the decrease in the tropical mean emission temperature. The net effect on the global methane flux of changes in wetland distribution varies among models, but is always small and cancels in the model mean.

[28] Emissions during the LGM are affected by the presence of ice sheets and newly exposed continental shelves, in addition to climatic and vegetation effects. Ice sheets reduce boreal emissions, while continental shelves are found to dominantly affect tropical emissions. Quantitative estimates of their separate impacts vary among models, but the combined effect on the global flux is consistently found to be small.

[29] Models simulate a shift from boreal wetlands to tropical wetlands, with the latter source becoming more important in the global methane budget during the LGM compared to the PIH. This is due to a slightly stronger reduction in boreal emissions (Figure 5), because the temperature sensitivity of the methane flux is higher at lower temperatures and because plant productivity decreases most at high northern latitudes. In addition, the geographic factors (ice sheets and shelves) shift emissions to the tropical zone. This simulated shift is consistent with the low interpolar gradient in atmospheric methane concentration that is derived from ice core data [*Chappellaz et al.*, 1997]. The present results do not support a complete shutdown of the boreal source, as postulated by *Fischer et al.* [2008]. Instead, they point to the importance of changes in wetland location for maintaining the boreal source at a significant level (9–19% of the total glacial wetland emissions).

[30] To summarize, we find a smaller reduction in the global methane flux than studies based on top-down modeling [e.g., *Crutzen and Brühl*, 1993; *Martinerie et al.*, 1995] but a larger reduction than recent studies using PMIP1-type simulations with Earth System models [*Kaplan*, 2002; *Valdes et al.*, 2005; *Kaplan et al.*, 2006]. The latter differ in a number of respects from the present PMIP2 simulations of climate during the LGM. First, they used an older ice sheet reconstruction in which the Fennoscandian ice sheet extended far east over northwestern

Siberia. This clearly resulted in a larger loss of potential wetland area. Second, the use of an improved ice sheet reconstruction [*Peltier*, 2004] and more sophisticated AO and AOV-GCMs in PMIP2 has resulted in some systematic differences in the simulated climate. Most notably, there is less continental drying over the NH extratropics and stronger cooling over the tropics in PMIP2 as compared to PMIP1 [*Braconnot et al.*, 2007a]. This has considerably improved model-data consistency. The simulated tropical cooling explains the strong reduction in the tropical wetland source in the present PMIP2-based estimates, as compared to earlier PMIP1-type studies, and hence the stronger global reduction.

[31] Variations in other methane sources than wetlands may have played a role too. Although ice core isotopic data suggest similar biomass burning during the LGM and PIH [*Fischer et al.*, 2008], charcoal data indicate that fire activity has increased considerably since the LGM [*Power et al.*, 2008]. Anthropogenic sources are likely to have been significant already during the PIH, given the size of the world population at that time (see the discussion by *Chappellaz et al.* [1997]). Finally, the relative reduction in the glacial atmospheric CH_4 concentration is expected to be somewhat larger than the relative reduction in the sources, because of chemical feedbacks [*Prather*, 1996] and other factors affecting CH_4 lifetime. Model studies find lifetime to be reduced by 10–20% during the LGM due to changes in the concentration of the hydroxyl radical OH and related gases [*Crutzen and Brühl*, 1993; *Martinerie et al.*, 1995] as well as reduced emissions of volatile organic compounds (VOCs) from terrestrial vegetation [*Valdes et al.*, 2005; *Kaplan et al.*, 2006].

[32] Considering anthropogenic and biomass burning sources together with the uncertainty in lifetime changes, the present PMIP2 based estimate of the glacial wetland source is easily reconciled with the observed drop in CH_4 concentration. More precise estimates could come from better constraints on methane lifetime, implying better constraints on factors that affect OH concentration (like relative humidity, temperature, UV radiation and clouds, and chemical species like O_3, NO_x and CO) as well as on glacial surface emissions of VOCs. Alternatively, future research might more fully exploit available ice core information by considering the methane evolution across the deglaciation, rather than only considering its LGM and PIH endpoints as in the present time-slice approach.

[33] **Acknowledgments.** We acknowledge the international modeling groups for providing their data for analysis and the Laboratoire des Sciences du Climat et de l'Environnement for collecting and archiving the model data. The PMIP2 Data Archive is supported by CEA, CNRS, the EU project MOTIF (EVK2-CT-2002-00153), and the Programme National d'Etude de la Dynamique du Climat.

References

Bergamaschi, P., et al. (2007), Satellite chartography of atmospheric methane from SCIAMACHY on board ENVISAT: 2. Evaluation based on inverse model simulations, *J. Geophys. Res.*, *112*, D02304, doi:10.1029/2006JD007268.

Braconnot, P., et al. (2007a), Results of PMIP2 coupled simulations of the Mid-Holocene and Last Glacial Maximum. Part 1: Experiments and large-scale features, *Clim. Past*, *3*, 261–277.

Braconnot, P., et al. (2007b), Results of PMIP2 coupled simulations of the Mid-Holocene and Last Glacial Maximum. Part 2: Feedbacks with emphasis on the location of the ITCZ and mid- and high latitudes heat budget, *Clim. Past*, *3*, 279–296.

Cao, M., S. Marshall, and K. Gregson (1996), Global carbon exchange and methane emissions from natural wetlands: Application of a process-based model, *J. Geophys. Res.*, *101*, 14,399–14,414.

Chappellaz, J. A., I. Y. Fung, and A. M. Thompson (1993), The atmospheric CH_4 increase since the Last Glacial Maximum, 1. Source estimates, *Tellus, Ser. B*, *45*, 228–241.

Chappellaz, J. A., T. Blunier, S. Kints, A. Dällenbach, J.-M. Barnola, J. Schwander, D. Raynaud, and B. Stauffer (1997), Changes in the atmospheric CH_4 gradient between Greenland and Antarctica during the Holocene, *J. Geophys. Res.*, *102*, 15,987–15,997, doi:10.1029/97JD01017.

Christensen, T. R., A. Ekberg, L. Ström, M. Mastepanov, N. Panikov, M. Öquist, B. H. Svensson, H. Nykänen, P. J. Martikainen, and H. Oskarsson (2003), Factors controlling large scale variations in methane emissions from wetlands, *Geophys. Res. Lett.*, *30*(7), 1414, doi:10.1029/2002GL016848.

Crutzen, P. J., and C. Brühl (1993), A model study of atmospheric temperatures and the concentrations of ozone, hydroxyl, and some other photochemically active gases during the glacial, the preindustrial Holocene and the present, *Geophys. Res. Lett.*, *20*, 1047–1050.

Farrera, I., et al. (1999), Tropical climates at the Last Glacial Maximum: A new synthesis of terrestrial paleoclimate data. 1. Vegetation, lake-levels and geochemistry, *Clim. Dyn.*, *15*, 823–856.

Fischer, H., et al. (2008), Changing boreal methane sources and constant biomass burning during the last termination, *Nature*, *452*, 864–867.

Gedney, N., P. M. Cox, and C. Huntingford (2004), Climate feedback from wetland methane emissions, *Geophys. Res. Lett.*, *31*, L20503, doi:10.1029/2004GL020919.

Houweling, S., F. Dentener, and J. Lelieveld (2000), Simulation of preindustrial atmospheric methane to constrain the global source strength of natural wetlands, *J. Geophys. Res.*, *105*, 17,243–17,255.

Kageyama, M., et al. (2006), LGM temperatures over the North Atlantic, Europe and western Siberia: a comparison between PMIP models, MARGO sea-surface temperatures and pollen-based reconstructions, *Quat. Sci. Rev.*, *25*, 2082–2102.

Kaplan, J. O. (2002), Wetlands at the Last Glacial Maximum: Distribution and methane emissions, *Geophys. Res. Lett.*, *29*(6), 1079, doi:10.1029/2001GL013366.

Kaplan, J. O., G. Folberth, and D. A. Hauglustaine (2006), Role of methane and biogenic volatile organic compound sources in late glacial and Holocene fluctuations of atmospheric methane concentrations, *Global Biogeochem. Cycles*, *20*, GB2016, doi:10.1029/2005GB002590.

Kohfeld, K. E., and S. P. Harrison (2000), How well can we simulate past climates? Evaluating the models using global paleoenvironmental datasets, *Quat. Sci. Rev.*, *19*, 321–346.

Lehner, B., and P. Döll (2004), Development and validation of a global database of lakes, reservoirs and wetlands, *J. Hydrol.*, *296*, 1–22, doi:10.1016/j.jhydrol.2004.03.028.

Martinerie, P., G. P. Brasseur, and C. Granier (1995), The chemical composition of ancient atmospheres: A model study constrained by ice core data, *J. Geophys. Res*, *100*, 14,291–14,304.

Matthews, E., and I. Y. Fung (1987), Methane emissions from natural wetlands: Global distribution, area, and environmental characteristics of sources, *Global Biogeochem. Cycles*, *1*, 61–86.

Peltier, W. R. (2004), Global glacial isostasy and the surface of the ice-age Earth: The ICE-5G (VM2) model and GRACE, *Annu. Rev. Earth Planet. Sci.*, *32*, 111–149.

Petit, J. R., et al. (1999), Climate and atmospheric history of the past 420,000 years from the Vostok ice core, Antarctica, *Nature*, *399*, 429–436.

Power, M. J., et al. (2008), Changes in fire regimes since the Last Glacial Maximum: An assessment based on a global synthesis and analysis of charcoal data, *Clim. Dyn.*, *30*, 887–907.

Prather, M. J. (1996), Timescales in atmospheric chemistry, *Geophys. Res. Lett.*, *23*, 2597–2600.

Prigent, C., F. Papa, F. Aires, W. B. Rossow, and E. Matthews (2007), Global inundation dynamics inferred from multiple satellite observations, 1993–2000, *J. Geophys. Res.*, *112*, D12107, doi:10.1029/2006JD007847.

Shindell, D. T., B. P. Walter, and G. Faluvegi (2004), Impacts of climate change on methane emissions from wetlands, *Geophys. Res. Lett.*, *31*, L21202, doi:10.1029/2004GL021009.

Thompson, R. S., and K. H. Anderson (2000), Biomes of western North America at 18000, 6,000, and 0 ^{14}Cyr BP reconstructed from pollen and packrat midden data, *J. Biogeogr.*, *27*, 555–584.

Valdes, P. J., D. J. Beerling, and C. E. Johnson (2005), The ice age methane budget, *Geophys. Res. Lett.*, *32*, L02704, doi:10.1029/2004GL021004.

Walter, B. P., M. Heimann, and E. Matthews (2001), Modeling modern methane emissions from natural wetlands: 1. Model description and results, *J. Geophys. Res.*, *106*, 34,189–34,206.

Weber, S. L., S. S. Drijfhout, A. Abe-Ouchi, M. Crucifix, M. Eby, A. Ganopolski, S. Murakami, B. Otto-Bliesner, and W. R. Peltier (2007), The modern and glacial overturning circulation in the Atlantic ocean in PMIP coupled model simulations, *Clim. Past*, *3*, 51–64.

Wu, H., J. Guiot, S. Brewer, and Z. Guo (2007), Climatic changes in Eurasia and Africa at the Last Glacial Maximum and mid-Holocene: Reconstruction from pollen data using inverse vegetation modelling, *Clim. Dyn.*, *29*, 211–229, doi:10.1007/s00382-007-0231-3.

A. J. Drury, W. H. J. Toonen, M. van Weele, and S. L. Weber, Royal Netherlands Meteorological Institute, PO Box 201, NL-3730 AE De Bilt, Netherlands. (weber@knmi.nl)